PHYSICAL REVIEW A **80**, 061605(R) (2009)

Polarization suppression and nonmonotonic local two-body correlations in the two-component Bose gas in one dimension

Jean-Sébastien Caux,[1] Antoine Klauser,[1,2] and Jeroen van den Brink[2,3]
[1]*Institute for Theoretical Physics, Universiteit van Amsterdam, 1018 XE Amsterdam, The Netherlands*
[2]*Instituut-Lorentz, Universiteit Leiden, P.O. Box 9506, 2300 RA Leiden, The Netherlands*
[3]*Leibniz-Institute for Solid State and Materials Research Dresden, D-01171 Dresden, Germany*
(Received 4 June 2009; published 14 December 2009)

We study the interplay of quantum statistics, strong interactions, and finite temperatures in the two-component (spinor) Bose gas with repulsive delta-function interactions in one dimension. Using the Thermodynamic Bethe Ansatz, we obtain the equation of state, population densities, and local density correlation numerically as a function of all physical parameters (interaction, temperature, and chemical potentials), quantifying the full crossover between low-temperature ferromagnetic and high-temperature unpolarized regimes. In contrast to the single component, Lieb-Liniger gas, nonmonotonic behavior of the local density correlation as a function of temperature is observed.

DOI: 10.1103/PhysRevA.80.061605 PACS number(s): 67.85.−d, 03.75.Kk, 05.30.Jp

The experimental realization of interacting quantum systems using cold atoms has reignited interest in many-body physics in and out of equilibrium [1]. Effectively one-dimensional (1D) bosonic ^{87}Rb quantum gases with tunable local interaction strength [2–6] realize the single-component Lieb-Liniger model [7,8], for which the crossover from weak to strong interactions is accessible and well understood. Observed thermodynamics [9] even fit predictions from the Thermodynamic Bethe Ansatz (TBA) [10]. For a single bosonic species in 1D, statistics and interactions are intimately related: the limit of infinitely strong interactions causes a crossover to effectively fermionic behavior [11,12] for density-dependent quantities. Density profiles and fluctuations accessible from exact thermodynamics allow to discriminate between these fermionized and quasicondensate regimes [13–16]. Multicomponent (spinor) systems however have many more regimes than their single-component counterparts, and realize situations where important interaction and quantum statistics effects coexist and compete. Their thermodynamics has not been extensively studied using exact methods; in this work, we wish to highlight some unexpected features inherent to such a system.

The experimentally realizable [17,18] case of two-component bosons in 1D with symmetric interactions, which we will focus on, contrasts with the Lieb-Liniger case in many ways. The ground state is polarized [19,20] (pseudospin ferromagnetic), as expected when spin-dependent forces are absent [21], and thus coincides with the Lieb-Liniger ground state. On the other hand, excitations carry additional branches, starting from the simplest spin-wavelike one. These excitations are difficult to describe, even in the strongly interacting limit (there, no fermionization can be used, since the two components remain strongly coupled), where spin-charge separation occurs [22–26]. The thermodynamic properties are drastically different from those of the Lieb-Liniger gas [27] and at large coupling and low temperature correspond to those of a *XXX* ferromagnetic chain [28]. Temperature suppresses the low-entropy polarized state, and opens up the possibility of balancing entropy and statistics gains (from the wave function symmetrization) with interaction and kinetic energy costs. Using a method based on integrability, we find that this thermally driven interplay leads to a correlated state with interesting features, the most remarkable being a nonmonotonic dependence of the local-density fluctuations with respect to temperature or relative chemical potential.

For definiteness, we consider a system of N particles on a ring of length L, subjected to the Hamiltonian

$$\mathcal{H}_N = -\frac{\hbar^2}{2m}\sum_{i=1}^{N}\frac{\partial^2}{\partial x_i^2} + g_{1D}\sum_{1\le i<j\le N}\delta(x_i - x_j). \tag{1}$$

The coupling g_{1D} is related to the effective 1D scattering length a_{1D} [29] via $g_{1D}=\hbar^2 a_{1D}/2m$, and to the interaction parameter $\gamma=c/n$ (where $n=N/L$ is the density) via $c=g_{1D}m/\hbar^2$. We set $\hbar=2m=1$. Yang and Sutherland [30,31] showed that the repulsive δ-interaction problem is exactly solvable irrespective of the symmetry of the wave function, so eigenstates of Eq. (1) are of Bethe Ansatz form whether the particles are distinguishable, or mixtures of bosons and fermions [32]. Multicomponent fermionic systems were studied by Schlottmann [33,34], but these results cannot be translated to the bosonic case we are interested in.

Specifically, specializing to N atoms of which M have (in the adopted cataloging) spin down, the Bethe Ansatz provides eigenfunctions fully characterized by sets of rapidities (quasimomenta) k_j, $j=1,\ldots,N$ and pseudospin rapidities λ_α, $\alpha=1,\ldots,M$, provided these obey the $N+M$ coupled Bethe equations [30,31].

$$e^{ik_jL} = -\prod_{l=1}^{N}\frac{k_j - k_l + ic}{k_j - k_l - ic}\prod_{\alpha=1}^{M}\frac{k_j - \lambda_\alpha - \frac{ic}{2}}{k_j - \lambda_\alpha + \frac{ic}{2}},$$

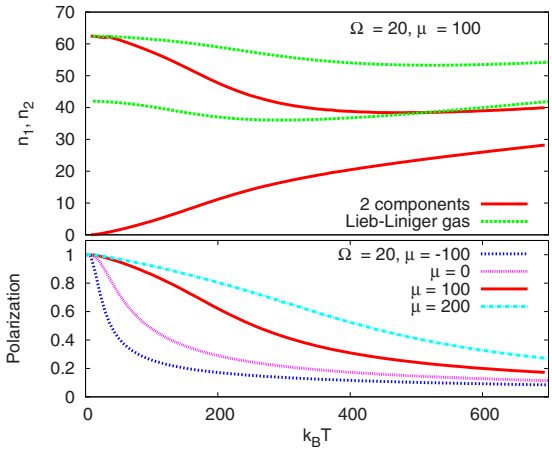

FIG. 1. (Color online) Population densities (top) and polarization (bottom) of the spinor Bose gas as a function of temperature, for fixed chemical potentials, and contrasted to separate Lieb-Liniger gases at corresponding chemical potentials. The Lieb-Liniger result for the majority chemical potential is recovered only at $T\to 0$, when ferromagnetism causes complete polarization.

$$\prod_{l=1}^{N}\frac{\lambda_\alpha - k_l - \frac{ic}{2}}{\lambda_\alpha - k_l + \frac{ic}{2}} = -\prod_{\beta=1}^{M}\frac{\lambda_\alpha - \lambda_\beta - ic}{\lambda_\alpha - \lambda_\beta + ic}, \tag{2}$$

for $j=1,\ldots,N$ and $\alpha=1,\ldots,M$. For a generic eigenstate, the solution to the Bethe equations is rather involved. In general, the k_j rapidities live on the real axis; the λ_α are on the other hand generically complex, but arranged into strings, each type representing a distinct quasiparticle. The spectrum of the theory contains infinitely many branches, with increasing effective mass. In the continuum limit $N\to\infty$, $L\to\infty$, N/L fixed, the TBA allows to exploit the condition of thermal equilibrium to obtain the Gibbs free energy as a function of the temperature T and of the total μ ($=\frac{\mu_1+\mu_2}{2}$ with μ_i the chemical potential specific to the ith component) and relative Ω ($=\frac{\mu_1-\mu_2}{2}$) chemical potentials. As detailed for example in [35] the Gibbs free energy density is given by

$$g = -T\int_{-\infty}^{\infty}\frac{dk}{2\pi}\ln[1+e^{-\epsilon(\lambda)/T}], \tag{3}$$

where $\epsilon(\lambda)$ is the dressed energy, which is coupled to the n-string dressed energy $\epsilon_n(\lambda)$, $n=1,2,\ldots$ via the system

$$\varepsilon(\lambda) = \lambda^2 - \mu - \Omega - Ta_2 * \ln[1+e^{-\varepsilon(\lambda)/T}] - T\sum_{n=1}^{\infty} a_n * \ln[1+e^{-\varepsilon_n(\lambda)/T}]$$

$$\frac{\varepsilon_1(\lambda)}{T} = f*\ln[1+e^{-\varepsilon(\lambda)/T}] + f*\ln[1+e^{\varepsilon_2(\lambda)/T}],$$

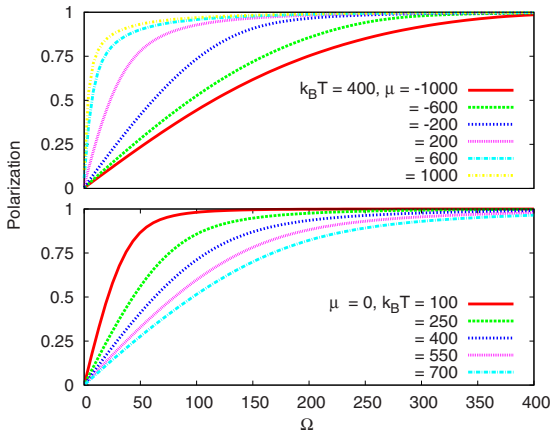

FIG. 2. (Color online) Polarization as a function of the relative chemical potential Ω, (top) at fixed temperature and for different values of the total chemical potential μ and (bottom) at fixed total chemical potential μ and for different temperatures.

$$\frac{\varepsilon_n(\lambda)}{T} = f*\ln[1+e^{\varepsilon_{n+1}(\lambda)/T}] + f*\ln[1+e^{\varepsilon_{n-1}(\lambda)/T}], \quad (n>1), \tag{4}$$

with the convolution $g*h(\lambda)\equiv\int_{-\infty}^{\infty}d\lambda' g(\lambda-\lambda')h(\lambda')$, and kernels $a_n(\lambda)=\frac{1}{\pi}\frac{nc/2}{(nc/2)^2+\lambda^2}$ and $f(\lambda)=\frac{1/2c}{\cosh(\pi\lambda/c)}$. This set of coupled equations is complemented with the asymptotic condition $\lim_{n\to\infty}\frac{\varepsilon_n(\lambda)}{n}=2\Omega$. In view of the absence of an analytical solution, we solve the infinite system of coupled integral equations numerically, representing a finite set of functions ε_n, $n=1,\ldots,n_{max}$. Functions with indices above n_{max} are replaced by their asymptotic value {obtainable from Eq. (4) by solving for constants $\varepsilon_n(\lambda\to\infty)\to\varepsilon_n^\infty$, see, e.g., [35]} and taken into account analytically. For each represented function, a finite interval in rapidity $|\lambda|<\lambda_n$ is used, and regions $|\lambda|>\lambda_n$ are again treated analytically using the asymptotic values above. Starting from an initial condition where $\varepsilon(\lambda)=\lambda^2-\mu-\Omega$ and all functions ε_n are set to their asymptotic value, we proceed iteratively, dynamically adjusting n_{max} and the integration limits as we go along in order to increase precision. In order to validate our results, we have in fact implemented two completely independent algorithms, one based on fast Fourier transforms and the other on adaptive-lattice Romberg-like integration. In order to compute the free energy, system Eq. (4) is implemented. In order to compute the free energy derivatives, coupled equations for the derivatives of the ε's [obtainable from (4)] are separately implemented (this gives much better accuracy than taking numerical derivatives of the original system). We have in any case verified that, e.g., $\frac{\Delta\varepsilon}{\Delta\mu}\equiv\frac{\varepsilon(\mu+\Delta\mu)-\varepsilon(\mu)}{\Delta\mu}\simeq\frac{\partial\varepsilon}{\partial\mu}$, the left-hand side being obtained from Eq. (4), the more accurate right-hand side by the equivalent implementation using analytical derivatives. While extremely challenging, it remains possible to obtain good accuracy (at least three digits) throughout parameter space, except in the extreme limit of vanishing relative chemical potential for $\Omega\ll T,\mu,c$ or the low-nonzero temperature limit $0<T\ll\Omega,\mu,c$ [36]. Leaving the details to

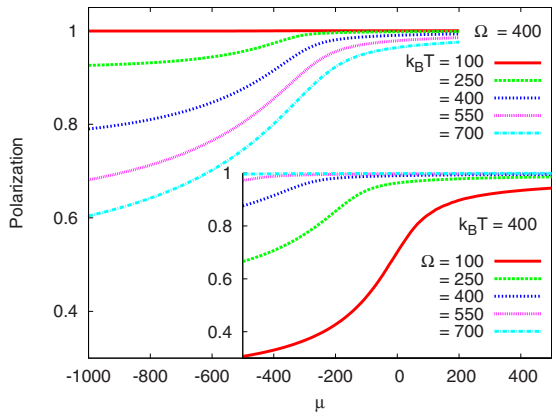

FIG. 3. (Color online) Polarization as a function of the total chemical potential μ, for fixed relative chemical potential Ω and for different temperatures (main) and (inset) for fixed temperature and for different values of the relative chemical potential Ω. Lowering the temperature or increasing Ω increases the polarization at any μ, leading back to Lieb-Liniger behavior.

a future publication, we here simply concentrate on the results obtained.

We focus on the polarization, defined as $(n_1-n_2)/(n_1+n_2)$ where $n_i=N_i/L$ the linear density of the ith boson component, and on the local density-density correlator $g^{(2)}=\frac{\Sigma_{i,j}\langle\Psi_i^\dagger\Psi_j^\dagger\Psi_j\Psi_i\rangle}{(\Sigma_i\langle\Psi_i^\dagger\Psi_i\rangle)^2}$. The linear densities together with other equilibrium quantities such as the entropy, will be discussed more extensively in a future publication. Figure 1 contrasts two single-component gases living in two different traps against cohabitation in the same trap, for a generic choice of chemical potentials. The polarization of the ground state is clearly visible and gets suppressed with temperature at a rate depending on μ, which itself sets the effective coupling γ. In the limit of $\mu \ll 0$, γ becomes bigger than $1/k_BT$, and the gas becomes paramagnetic. For $\mu \gg 0$ ($\gamma \ll 1$), the gas shows ferromagnetic behavior. The effect of the relative chemical potential on the polarization is shown in Fig. 2. Due to the

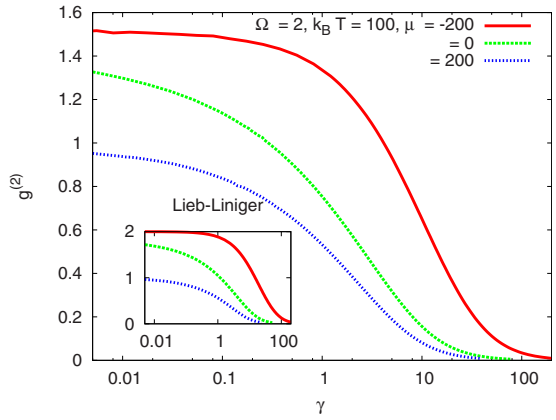

FIG. 4. (Color online) Local pair correlation $g^{(2)}$ of the spinor Bose gas as a function of the effective coupling γ, at fixed temperature and for three different values of the total chemical potential μ. The relative chemical potential Ω is set to a low value. Inset: the same curves for the Lieb-Liniger gas. The asymptotes $\gamma \to 0$ differ, but the general shape of the curve is very similar.

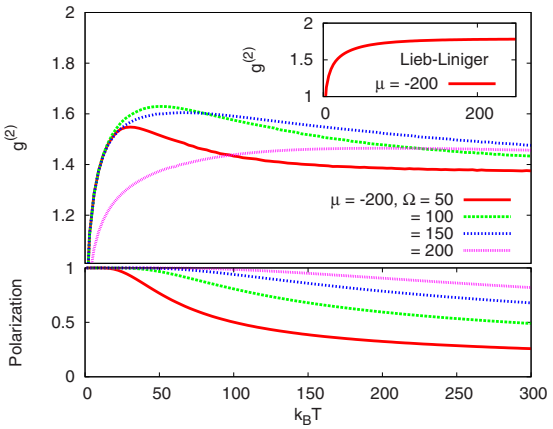

FIG. 5. (Color online) Top: local pair correlation $g^{(2)}$ as a function of temperature, for fixed total chemical potential μ and four different values of the relative chemical potential Ω. The nonmonotonicity of $g^{(2)}$ in the spinor gas is to be contrasted to its monotonicity in the Lieb-Liniger case (top, inset). Bottom: polarization as a function of T, for the same values of Ω and μ. At zero temperature, polarization is total irrespective of the chemical potential (see also Fig. 1), illustrating the ferromagnetic-like physics involved in the spinor gas.

finite temperature, the limit $\Omega \to 0$ is always unpolarized. Figure 3 shows data for a wide range of the total chemical potential. For μ small enough ($\gamma \gg 1$, paramagnetic), the value of the polarization depends only on Ω and T. In contrast, for $\mu \gg 0$, the system behaves as a quasicondensate ($\gamma \ll 1$, ferromagnetic).

The observable $g^{(2)}$, which can be obtained from the interaction parameter derivative of Eq. (3), quantifies the fluctuations of density at a local point. Figure 4 presents data for this as a function of γ. In the limit $\gamma \to 0$ and in the decoherent regime (where the reduced temperature $\tau \equiv \frac{T}{(n_1+n_2)^2} \gg 1$), the value saturates between 2 (for $\Omega \to \infty$) and $1+\frac{1}{N_c}$ (for $\Omega \to 0$, where $N_c=2$ is the number of components), generalizing the Lieb-Liniger result [15]. Our data fit well with

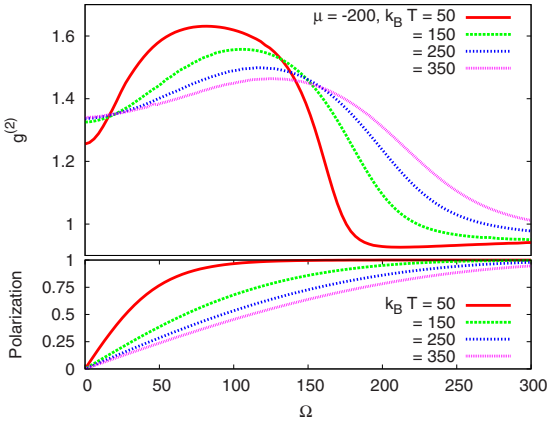

FIG. 6. (Color online) Top: the local pair correlation $g^{(2)}$ as a function of the relative chemical potential Ω, for fixed total chemical potential μ and four different values of the temperature. Bottom: polarization as a function of the relative chemical potential, for the same values of T and μ.

this prediction, as seen in Fig. 4, where for $\gamma \sim 10^{-2}$, $g^{(2)}$ approaches 1.5 for Ω and μ small. For bigger μ, the data do not reach this value since the reduced temperature is too low and the decoherent regime is not yet reached. When the gas becomes strongly interacting, $g^{(2)}$ vanishes as expected.

When studied as a function of temperature, the behavior of $g^{(2)}$ is markedly different in the two-component gas than in the single-component case. For fixed chemical potentials, it can exhibit a maximum at finite temperature as shown in Fig. 5. In the regime of large relative chemical potential, the gas is polarized and $g^{(2)}$ is monotonic in T; however, one can clearly observe that for $\Omega \to 0$ a peak appears. For this range of temperatures, τ is >1 but γ passes from high values at low T to almost zero for high T. As a function of Ω (Fig. 6), $g^{(2)}$ exhibits a maximum followed by a local minimum. The gas is in the decoherent regime at small Ω and the saturation value of the correlation for this regime increases with Ω. For bigger values $1 \gg \gamma \gg \tau$ and for $\Omega \geq \mu$, the first component is quasicondensating and $g^{(2)} \sim 1$.

The existence of a maximum and minimum of the density fluctuations is the result of an interesting competition between interaction energy and entropy. On the one hand, the bosonic nature favors ferromagnetic correlations, which in general set the small-temperature thermodynamic properties. On the other hand, the reduced entropy associated with the polarized states and the enhanced spatial density resulting from quasicondensation bear a free-energy cost which can or cannot be afforded depending on the value of temperature and of the chemical potentials. Our work clarifies and quantifies these effects fully throughout the available parameter space: depending on the precise values of these three parameters, we see that the system equilibrates to a state with markedly differing correlations. As a corollary, the nonmonotonicity found in $g^{(2)}$ could point to other interesting consequences for realizations of such a system. The population densities of a two-component Bose gas in a trap, obtainable by coupling our method to a local-density approximation, would also display correlated behavior as a function of position. The ferromagnetic tendencies of the system would tend to drive phase separation, leading to an observable enhancement and depletion of the spatial density profiles of the different bosonic species.

The authors would like to thank N. J. van Druten and G. V. Shlyapnikov for stimulating discussions, and gratefully acknowledge support from the FOM Foundation.

[1] I. Bloch, J. Dalibard, and W. Zwerger, Rev. Mod. Phys. **80**, 885 (2008).
[2] H. Moritz, T. Stöferle, M. Köhl, and T. Esslinger, Phys. Rev. Lett. **91**, 250402 (2003).
[3] B. Laburthe Tolra *et al.*, Phys. Rev. Lett. **92**, 190401 (2004).
[4] B. Paredes *et al.*, Nature (London) **429**, 277 (2004).
[5] T. Kinoshita, T. Wenger, and D. S. Weiss, Science **305**, 1125 (2004).
[6] L. Pollet, S. M. A. Rombouts, and P. J. H. Denteneer, Phys. Rev. Lett. **93**, 210401 (2004).
[7] E. H. Lieb and W. Liniger, Phys. Rev. **130**, 1605 (1963).
[8] E. H. Lieb, Phys. Rev. **130**, 1616 (1963).
[9] A. H. van Amerongen, J. J. P. van Es, P. Wicke, K. V. Kheruntsyan, and N. J. van Druten, Phys. Rev. Lett. **100**, 090402 (2008).
[10] C. N. Yang and C. P. Yang, J. Math. Phys. **10**, 1115 (1969).
[11] L. Tonks, Phys. Rev. **50**, 955 (1936).
[12] M. Girardeau, J. Math. Phys. **1**, 516 (1960).
[13] D. S. Petrov, G. V. Shlyapnikov, and J. T. M. Walraven, Phys. Rev. Lett. **85**, 3745 (2000).
[14] D. M. Gangardt and G. V. Shlyapnikov, Phys. Rev. Lett. **90**, 010401 (2003).
[15] K. V. Kheruntsyan, D. M. Gangardt, P. D. Drummond, and G. V. Shlyapnikov, Phys. Rev. Lett. **91**, 040403 (2003).
[16] K. V. Kheruntsyan, D. M. Gangardt, P. D. Drummond, and G. V. Shlyapnikov, Phys. Rev. A **71**, 053615 (2005).
[17] A. Widera *et al.*, Phys. Rev. Lett. **100**, 140401 (2008).
[18] S. Palzer, C. Zipkes, C. Sias, and M. Köhl, Phys. Rev. Lett. **103**, 150601 (2009).
[19] B. Sutherland, *Beautiful Models* (World Scientific, Singapore, 2004).
[20] K. Yang and Y. Q. Li, Int. J. Mod. Phys. B **17**, 1027 (2003).
[21] E. Eisenberg and E. H. Lieb, Phys. Rev. Lett. **89**, 220403 (2002).
[22] J. N. Fuchs, D. M. Gangardt, T. Keilmann, and G. V. Shlyapnikov, Phys. Rev. Lett. **95**, 150402 (2005).
[23] Y.-Q. Li, S.-J. Gu, Z.-J. Ying, and U. Eckern, Europhys. Lett. **61**, 368 (2003).
[24] M. T. Batchelor, M. Bortz, X. W. Guan, and N. Oelkers, J. Stat. Mech.: Theory Exp. 2006, P03016 (2006).
[25] M. B. Zvonarev, V. V. Cheianov, and T. Giamarchi, Phys. Rev. Lett. **99**, 240404 (2007).
[26] A. Kleine, C. Kollath, I. P. McCulloch, T. Giamarchi, and U. Schollwöck, New J. Phys. **10**, 045025 (2008).
[27] S.-J. Gu, Y.-Q. Li, Z.-J. Ying, and X.-A. Zhao, Int. J. Mod. Phys. B **16**, 2137 (2002).
[28] X.-W. Guan, M. T. Batchelor, and M. Takahashi, Phys. Rev. A **76**, 043617 (2007).
[29] M. Olshanii, Phys. Rev. Lett. **81**, 938 (1998).
[30] C. N. Yang, Phys. Rev. Lett. **19**, 1312 (1967).
[31] B. Sutherland, Phys. Rev. Lett. **20**, 98 (1968).
[32] M. Gaudin, *La Fonction d'onde de Bethe* (Masson, Paris, 1983).
[33] P. Schlottmann, J. Phys.: Condens. Matter **5**, 5869 (1993).
[34] P. Schlottmann, J. Phys.: Condens. Matter **6**, 1359 (1994).
[35] M. Takahashi, *Thermodynamics of One-Dimensional Solvable Models* (Cambridge University Press, Cambridge, England, 1999).
[36] Because of the covariance of the theory under overall rescaling of T, μ, Ω, and c, we can always set $c=1$.